



Marburg Virus and Risk Factor Among Infected Population: A Modeling Study

Haque, Z.^{1,4}, Kamrujjaman, M.*¹, Alam, M. S.², and Biswas, M. H. A.³

¹*Department of Mathematics, University of Dhaka, Dhaka-1000, Bangladesh*

²*Department of Mathematics, University of Houston, Houston, Texas- 77204, USA*

³*Mathematics Discipline, Khulna University, Khulna-9208, Bangladesh*

⁴*Department of Mathematics, American International University-Bangladesh, Dhaka, Bangladesh*

E-mail: kamrujjaman@du.ac.bd

**Corresponding author*

Received: 30 October 2023

Accepted: 1 January 2024

Abstract

This study aims to investigate the role of individuals with natural immunity in contributing to the overall spread of Marburg virus infection, a highly lethal human pathogen. Marburg virus was initially identified in 1967 during a significant outbreak in Marburg, Germany, and Belgrade, Serbia. Notably, there are currently no approved vaccines or treatments for Marburg virus infection due to its alarmingly high fatality rate. The study developed a mathematical model to better understand the transmission dynamics of Marburg virus disease (MVD), specifically focusing on the spread of infected individuals. Initial analysis employed established methods, evaluating factors such as the positive assessments, the basic reproduction number, and equilibrium point stability. This analytical approach provided valuable insights into MVD dynamics. Following this, numerical simulations were conducted to visually depict the outcomes derived from the analytical analysis. These simulations provided a more comprehensive understanding of the complex dynamics of MVD. Finally, this study presents a comprehensive analysis of Marburg virus transmission dynamics, shedding light on the impact of natural immunity on disease spread and emphasizing the significance of isolation strategies in mitigating the outbreak of this highly lethal pathogen.

Keywords: MVD; natural immunity system; mathematical model; stability; numerical simulations.

1 Introduction

Marburg Virus Disease (MVD) is caused by the Marburg virus, which is part of the Filoviridae family, the same family as the Ebola virus. MVD is a rare but highly virulent disease that can cause severe outbreaks and has been the source of several disasters in the past. MVD, an exceedingly rare but deadly illness, has been a subject of global concern since its discovery in Europe in 1967. While its impact has been mainly concentrated in East Africa, the Marburg virus's swift transmission and high fatality rates have led the World Health Organization (WHO) to designate it as a priority pathogen. This article explores the features of MVD, including its transmission, effects, and the urgent necessity for prevention. It emphasizes a groundbreaking mathematical modeling approach intended to eliminate the disease entirely. MVD denotes Marburg virus disease, caused by the Marburg virus (MARV). This virus was first identified in Europe in 1967, marking its ominous debut on the global stage. Subsequently, the majority of MVD incidents have occurred in East Africa [20]. MVD is exceptionally rare, and it is essential to understand that it is not an airborne disease; thus, it does not easily spread through respiratory droplets. Marburg virus, a known toxin, has been classified as a priority pathogen by the WHO due to its potential for rapid transmission and severe outcomes [6].

The WHO categorizes MVD as "epidemic-prone," signifying that it can readily spread among humans if preventive measures are not implemented. However, the exact mechanism by which the Marburg virus initially jumps from its animal host to humans remains a mystery. Transmission of the Marburg virus happens through direct contact with bodily fluids, such as blood, urine, saliva, sweat, feces, vomit, breast milk, and amniotic fluid. Moreover, the virus can also be transmitted through mucous membranes in the eyes, nose, or mouth when they come into contact with individuals who are either afflicted by or have succumbed to MVD [25]. Importantly, there is currently no documented evidence of Marburg virus transmission through sexual contact or contact with vaginal fluids from women who have had MVD. In light of the lack of an authorized treatment or vaccine for MVD, prevention becomes of utmost importance. Practices such as employing personal protective equipment (PPE) and maintaining secure handling of bodily fluids are crucial. Diagnosing MVD can be accomplished through diverse methods, such as culture, reverse transcription polymerase chain reaction (RT-PCR), serology, and immunohistochemistry. The selection of the method relies on the infection stage [25]. Common diagnostic samples encompass blood, other bodily fluids, and tissue obtained during autopsies, with a positive test confirming the current infection. The Marburg virus is considered zoonotic, and it is naturally maintained in Egyptian fruit bats (*Rousettus aegyptiacus*), which are widely distributed throughout Africa [21]. In the early stages of infection, individuals might exhibit symptoms like nausea, vomiting, chest discomfort, a sore throat, abdominal pain, and diarrhea. As the disease progresses, these symptoms intensify and may lead to more severe conditions, including jaundice, pancreas inflammation, substantial weight loss, delirium, shock, liver failure, extensive bleeding, and the dysfunction of multiple organs.

The impact of MVD has been devastating in past outbreaks. For instance, during the 1998-2000 outbreak in the Democratic Republic of Congo (DRC), the case fatality rate was a staggering 83% [2]. Similarly, in the 2004–2005 outbreak in Angola, the fatality rate reached a harrowing 90%. The most significant and deadliest outbreak occurred in northern Angola in 2005 [1]. The severity of these outbreaks underscores the urgency of addressing MVD. While historically, MVD outbreaks have primarily occurred in East Africa, instances of the disease have been identified in other parts of the world. On January 9, 2008, a case of an unexplained febrile illness that necessitated hospitalization was detected by the Colorado Department of Public Health and Environment (CDPHE) in a woman who had recently returned from a trip to Uganda [13]. In Uganda, the outbreak spanning from 2007 to 2017 witnessed a rapid surge in the mortality rate. Likewise, in July 2008, a

case of MHF (Marburg hemorrhagic fever) was diagnosed in the Netherlands, stemming from an imported infection [22].

However, the most recent development in the MVD landscape is the initial occurrence of the disease in West Africa, specifically in Guinea, in 2021 [12]. On June 28, 2022, two tragic instances of Marburg virus disease were recorded in the Ashanti region of Ghana. Addressing these cases and preventing further outbreaks is of paramount importance due to the Marburg virus's potential for rapid transmission. The ambitious yet vital goal of eradicating Marburg virus disease (MVD) from the face of the Earth is underscored by the localized nature of the outbreaks, primarily within the African continent, presenting a unique opportunity for containment and eradication. To achieve this goal, a multifaceted approach is imperative. Given the potential for rapid transmission, addressing these cases and preventing further outbreaks is of paramount importance. Eradicating Marburg virus disease from the face of the Earth is an ambitious but vital goal. Given the localized nature of the outbreaks, primarily within the African continent, it presents a unique opportunity for containment and eradication. To achieve this goal, a multifaceted approach is imperative.

- Careful isolation of infected individuals from those who have been exposed is a fundamental step in reducing the rate of infection. Quick identification and isolation can prevent further transmission.
- Safe and hygienic burial practices are essential in controlling the outbreak. Handling the deceased with proper protective measures reduces the risk of transmission.
- Implementing a robust contact tracing strategy at the earliest signs of an outbreak is crucial. Identifying and monitoring individuals who may have been exposed can significantly reduce the spread of MVD.
- Educating the public about the risks and prevention of MVD is key. Knowledge empowers individuals to protect themselves and take necessary precautions.
- Invest in research to develop an effective vaccine and treatment for MVD. This will not only save lives but also serve as a long-term solution. To further support eradication efforts, a mathematical modeling approach has been employed to study the dynamics of MVD from 2000 to 2022, providing insights into key epidemiological parameters and offering a framework for effective intervention strategies. The primary goal of this study is to formulate strategies to eliminate MVD from the world. This mathematical model provides insights into the key epidemiological parameters of MVD and offers a framework for developing effective intervention strategies. The mathematical model employs a compartmental approach to understand the progression of MVD. Over the years of study, the simulation demonstrates promising results. Recovered individuals are on the rise, while the number of infected individuals decreases. This outcome is a testament to the efficacy of early intervention, isolation, and other eradication measures.

Marburg Virus Disease is a rare but deadly illness with the potential to cause significant harm if left unchecked. While its historical epicenters have been primarily in East Africa, recent cases in other parts of the world underscore the need for global awareness and collaborative efforts to eradicate the disease. The combination of prevention, early isolation, safe burial practices, contact tracing, public awareness, research, and vaccination development is essential for bringing an end to MVD [24]. The use of mathematical modeling provides a valuable tool for understanding the disease's dynamics and formulating strategies for eradication. With continued vigilance and global cooperation, there is hope that Marburg Virus Disease can be consigned to the annals of history, ensuring a safer and healthier world for all.

Background of MVD in Africa

Marburg virus disease (MVD) is a severe and highly contagious illness caused by the Marburg virus, a member of the Marburg virus genus within the Filoviridae family. It shares several characteristics with its infamous relative, the Ebola virus, and is responsible for acute hemorrhagic fever in both humans and non-human primates [10, 15]. While Marburg virus disease has not yet evolved into a worldwide pandemic, it has remained largely contained within the African continent. In this article, we will delve into the background of Marburg virus disease and discuss recent insights gained from analyzing data collected by the World Health Organization (WHO) [3, 23, 26].

The understanding of MVD symptoms primarily arises from clinical data collected during three significant outbreaks in history. These outbreaks include the 1967 occurrences in Germany and Yugoslavia, the 1998-2000 outbreak in the Democratic Republic of Congo, and the 2004-2005 outbreak in Angola. These events offered valuable insights into the disease's clinical presentation and progression. It is worth noting that despite variations in case fatality rates, the clinical symptoms observed in different outbreaks have largely remained consistent [10].

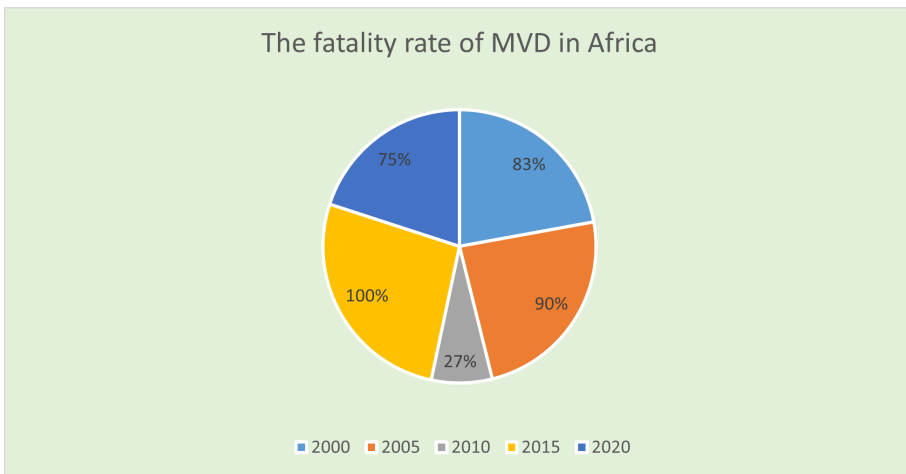


Figure 1: The pandemic situation of MVD in Africa.

Figure 1, as presented in this context, highlights a noteworthy observation. In the year 2010, MVD experienced its lowest fatality rate, indicating potential advancements in medical care, treatment strategies, or other factors that contributed to a decrease in mortality. However, this is only a glimpse of the broader picture. The data collected from WHO is instrumental in helping experts understand the dynamics of MVD and its possible evolution. This information is not only valuable in retrospective analysis but also for predicting future trends and helping with preparedness and response measures. While MVD has not reached global pandemic proportions, its potential for rapid transmission and high mortality rates make it a concern for public health. As we continue to learn more about the Marburg virus and MVD through data analysis and research, we can work towards more effective prevention and treatment strategies. Moreover, this knowledge contributes to our understanding of the broader field of emerging infectious diseases and how they can impact human populations.

Marburg virus disease continues to pose a significant threat predominantly in the African continent, marked by occasional outbreaks. The examination of clinical data from past outbreaks, as

depicted in Figure 1, emphasizes the criticality of monitoring and comprehending the disease’s advancement. With this knowledge, public health organizations and medical researchers can develop strategies to control and ultimately eliminate the threat of MVD and other emerging infectious diseases. The current study centers on a five-compartment mathematical model designed to visualize the propagation of the MVD virus and explore strategies to control the spread of the disease. Biomedical models facilitate the assessment of various intervention strategies’ effectiveness, such as vaccination campaigns, isolation protocols, or treatment strategies. They underscore the significance of early detection, isolation of infected individuals, and contact tracing.

2 Formulation and Mathematical Model

In this study, we have developed a five-compartmental model for Marburg virus disease (MVD), illustrating the frequency at which populations are impacted. Let the first compartment $S(t)$ denotes susceptible populations, exposed $E(t)$, isolated individuals $I_{so}(t)$ with natural immunity and infected individuals $I_{nf}(t)$ with weak immunity, recovered $R(t)$. In order to address the lack of targeted treatment for Marburg virus disease, it is vital for individuals with severe cases should to be provided with supportive care in a hospital environment. Some infected populations are dying at the rate μ , natural death is considered at the rate δ_0 which is negligible, infected populations are recovered at the rate r and very small. The interconnected transmissions among various compartments are depicted in Figure 2.

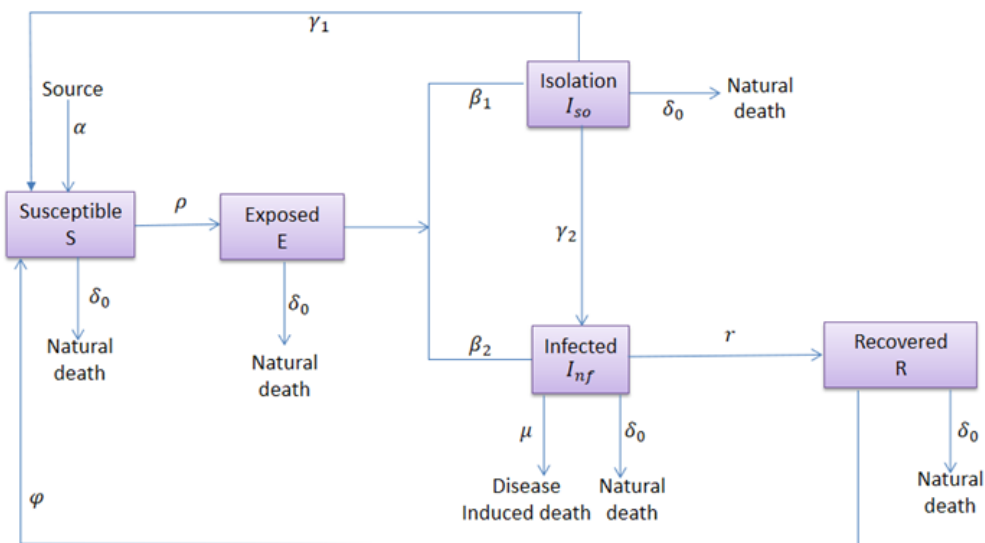


Figure 2: Disease transmission diagram of five compartmental MVD model.

The proposed model can be represented by:

$$\begin{aligned}
 \frac{dS(t)}{dt} &= \alpha + \gamma_1 I_{so} + \varphi R - \rho SE - \delta_0 S, \\
 \frac{dE(t)}{dt} &= \rho SE - \beta_1 E - \beta_2 E - \delta_0 E, \\
 \frac{dI_{so}(t)}{dt} &= \beta_1 E - \gamma_1 I_{so} - \gamma_2 I_{so} - \delta_0 I_{so}, \\
 \frac{dI_{nf}(t)}{dt} &= \beta_2 E + \gamma_2 I_{so} - r I_{nf} - \mu_0 I_{nf} - \delta_0 I_{nf}, \\
 \frac{dR(t)}{dt} &= r I_{nf} - \varphi R - \delta_0 R.
 \end{aligned} \tag{1}$$

Given the following initial conditions,

$$S(0) = S_0 > 0, \quad E(0) = E_0 > 0, \quad I_{so}(0) = I_{0so} > 0, \quad I_{nf}(0) = I_{0nf} > 0, \quad R(0) = R_0 > 0.$$

In these equations, all the parameters are positive; we have assumed stable population with per capita birth rate α and per capita death rate μ (disease induced death rate is considered in the system) β_1 is the isolation rate and β_2 is the infection rate of exposed population and r is spontaneous recovery rate of infected individuals. γ_1 is the rejoining rate of isolation individuals to susceptible individuals and γ_2 is the rate at which the isolated individuals get infected with Marburg virus. δ_0 is the natural death rate and φ is the rejoining rate of recovered individuals to susceptible individuals.

The mathematical model holds significant clinical relevance in controlling the Marburg virus and similar infectious diseases. The proposed five compartments model helps in understanding the progression of an infectious disease like Marburg virus by dividing the population into compartments representing different stages of infection. This understanding aids in predicting how the disease spreads through a population over time. By using the modeling concepts, researchers can simulate various intervention strategies such as vaccination campaigns, quarantine measures, or public health interventions. These simulations can predict the potential impact of these strategies on disease spread, assisting in determining the most effective control measures.

3 Mathematical Evaluation of the Marburg Virus Disease (MVD) Model

Within this section, we explore the aspects of boundedness, positivity, equilibrium analysis, the stability of equilibrium points, and the calculation of the basic reproduction number for the model.

Boundedness of solutions

Here we show that, the total population is bounded for all $t \geq 0$.

Theorem 3.1. *The region $\phi = \{(S(t), E(t), I_{so}(t), I_{nf}(t), R(t)) \in \mathbb{R}_+^5\}$ remains a positively invariant set in the context of the proposed models.*

Proof. Assuming the total population, $N(t)$ where, $N(t) = S(t) + E(t) + I_{so}(t) + I_{nf}(t) + R(t)$. In

that case, the rate of change is

$$\begin{aligned} \frac{dN}{dt} &= \frac{dS}{dt} + \frac{dE}{dt} + \frac{I_{so}}{dt} + \frac{dI_{nf}}{dt} + \frac{dR}{dt}, \\ \Rightarrow \frac{dN}{dt} &= \alpha + \gamma_1 I_{so} + \varphi R - \rho SE - \delta_0 S + \rho SE - \beta_1 E - \beta_2 E - \delta_0 E + \beta_1 E - \gamma_1 I_{so} \\ &\quad - \gamma_2 I_{so} - \delta_0 I_{so} + \beta_2 E + \gamma_2 I_{so} - r I_{nf} - \mu_0 I_{nf} - \delta_0 I_{nf} + r I_{nf} - \varphi R - \delta_0 R, \\ \Rightarrow \frac{dN}{dt} &= \alpha - \delta_0 N - \mu I_{nf}. \end{aligned}$$

Since $N(t)$ is assumed to be constant over a time t , we have

$$\frac{dN}{dt} = \alpha - \delta_0 N - \mu I_{nf} = 0.$$

If disease induced death is zero, then $\alpha - \delta_0 N \leq 0$, so $N(t) \leq \frac{\alpha}{\delta_0}$.

For all $t \geq 0$, $\phi = \left\{ (S(t), E(t), I_{so}(t), I_{nf}(t), R(t)) \in \mathbb{R}_+^5 : N(t) \leq \frac{\alpha}{\delta_0} \right\}$,

i.e., $\frac{\alpha}{\delta_0}$ is the upper bound of $N(t)$. Conversely, if $N(t) \geq \frac{\alpha}{\delta_0}$, then $N(t)$ will decrease to $\frac{\alpha}{\delta_0}$.

As $t \rightarrow \infty$, the solutions $(S(t), E(t), I_{so}(t), I_{nf}(t), R(t))$ enters the region ϕ or it approaches it asymptotically. Therefore, the model is well-posed both mathematically and epidemiologically within the defined region. \square

Positivity of the Model

Given that the proposed model describes the human population, it is imperative to establish the non-negativity of all variables employed in the model.

Theorem 3.2. *If $S(t) \geq 0, E(t) \geq 0, I_{so}(t) \geq 0, I_{nf}(t) \geq 0, R(t) \geq 0$, then the solution of the system is positive.*

Proof. We recall the first equation of the model equation (1),

$$\frac{dS(t)}{dt} = \alpha + \gamma_1 I_{so} + \varphi R - \rho SE - \delta_0 S. \tag{2}$$

To find the positivity of the equation (2), we have

$$\begin{aligned} \frac{dS(t)}{dt} &\geq \alpha - \delta_0 S, \\ \Rightarrow \frac{dS(t)}{dt} + \delta_0 S &\geq \alpha. \end{aligned} \tag{3}$$

Integrating equation (3), we have

$$S(t) \geq \frac{\alpha}{\delta_0} + ce^{-\delta_0 t}, \quad c = \text{integrating constant.} \tag{4}$$

Applying initial condition at $t = 0$, $S(0) - \frac{\alpha}{\delta_0} \geq c$. From equation (4), we get

$$S(t) \geq \frac{\alpha}{\delta_0} + \left(S(0) - \frac{\alpha}{\delta_0} \right) e^{-\delta_0 t}$$

whenever $t = 0$ and $t \rightarrow \infty$, $S(t) > 0$. By replicating the aforementioned procedure, we can demonstrate the positivity of all other state variables. Therefore, it is evident that for all $t \geq 0$, $S(t) > 0$, $E(t) > 0$, $I_{so}(t) > 0$, $I_{nf}(t) > 0$, $R(t) > 0$.

Hence the positivity of our proposed model is proved. □

4 Equilibrium Points and Basic Reproduction Number

The disease-free equilibrium (DFE) is characterized by the absence of the disease within the population. To identify the disease-free equilibrium point for the model described in equation (1), we must solve

$$\frac{dS}{dt} = \frac{dE}{dt} = \frac{dI_{so}}{dt} = \frac{dI_{nf}}{dt} = \frac{dR}{dt} = 0. \tag{5}$$

Since there is no infection for DFE point, we obtain

$$E = 0, \quad I_{so} = 0, \quad I_{nf} = 0, \quad R = 0.$$

Now putting these values in the first equation of the model equation (1)

$$\begin{aligned} \alpha - \delta_0 S &= 0, \\ \Rightarrow S &= \frac{\alpha}{\delta_0}. \end{aligned}$$

Hence, the DFE point of the model equation (1) is $E_{dfe} \left(\frac{\alpha}{\delta_0}, 0, 0, 0, 0 \right)$.

The Endemic equilibrium point (EEP) is a state where the disease cannot be completely eliminated but persists within the population. To determine the EEP (W^*) of the problem, one can yields,

$$\frac{dS}{dt} = \frac{dE}{dt} = \frac{dI_{so}}{dt} = \frac{dI_{nf}}{dt} = \frac{dR}{dt} = 0. \tag{6}$$

From the second equation of the model (1),

$$\frac{dE(t)}{dt} = \rho S^* E - \beta_1 E - \beta_2 E - \delta_0 E = 0,$$

which implies,

$$S^* = \frac{\beta_1 + \beta_2 + \delta_0}{\rho} = \frac{A_3}{\rho}.$$

From the third equation of the model (1),

$$\frac{dI_{so}}{dt} = \beta_1 E^* - \gamma_1 I_{so}^* - \gamma_2 I_{so}^* - \delta_0 I_{so}^* = 0.$$

such that,

$$I_{so}^* = \frac{\beta_1 E^*}{\gamma_1 + \gamma_2 + \delta_0} = \frac{\beta_1 E^*}{A_1}.$$

Similarly, fourth and fifth equation ensures,

$$\begin{aligned} I_{nf}^* &= \frac{(A_1\beta_2 + \gamma_2\beta_1) E^*}{A_1 A_2}, & A_2 &= r + \mu + \delta_0, \\ R^* &= \frac{r E^* (A_1\beta_2 + \gamma_2\beta_1)}{A_1 A_2 A_4}, & A_4 &= \varphi + \delta_0. \end{aligned}$$

From the first equation of the model (1),

$$\begin{aligned} \frac{dS}{dt} &= \alpha + \gamma_1 I_{so}^* + \varphi R^* - \rho S^* E^* - \delta_0 S^* = 0, \\ \Rightarrow E^* &= \frac{(\delta_0 A_3 - \alpha \rho) A_1 A_2 A_4}{(r\varphi(A_1\beta_2 + \gamma_2\beta_1) + A_2 A_4 \gamma_1 \beta_1 - A_1 A_2 A_3 A_4) \rho}, \end{aligned}$$

so,

$$\begin{aligned} W^*(S^*, E^*, I_{so}^*, I_{nf}^*, R^*) &= \left(\frac{A_3}{\rho}, \frac{(\delta_0 A_3 - \alpha \rho) A_1 A_2 A_4}{(r\varphi(A_1\beta_2 + \gamma_2\beta_1) + A_2 A_4 \gamma_1 \beta_1 - A_1 A_2 A_3 A_4) \rho}, \frac{\beta_1 E^*}{A_1}, \right. \\ &\quad \left. \frac{(A_1\beta_2 + \gamma_2\beta_1) E^*}{A_1 A_2}, \frac{r E^* (A_1\beta_2 + \gamma_2\beta_1)}{A_1 A_2 A_4} \right). \end{aligned}$$

The fundamental reproduction number (R_0), alternatively known as the basic reproduction ratio or rate, or simply the basic reproductive rate, serves as a key epidemiological measure employed to characterize the infective or transmissible of infectious agents. The value of R_0 provides valuable insights into the level of intervention required to either thwart an epidemic or eradicate an infection within a specific population. Therefore, estimating R_0 for a particular disease within a given population is of paramount importance.

Basic Reproduction Number R_0 at DFE

Here we will use next generation matrix to compute R_0 . Let F_i represent the rate at which new infections appear, and V_i denote the rate at which individuals exit the respective compartments,

$$F_i = \begin{bmatrix} F_1 \\ F_2 \\ F_3 \end{bmatrix} = \begin{bmatrix} \rho S E \\ \beta_1 E \\ \gamma_2 I_{so} + \beta_2 E \end{bmatrix}, \text{ and } V_i = \begin{bmatrix} V_1 \\ V_2 \\ V_3 \end{bmatrix} = \begin{bmatrix} c(\beta_1 + \beta_2 + \delta_0) E \\ (\gamma_1 + \gamma_2 + \delta_0) I_{so} \\ (\mu + r + \delta_0) I_{nf} \end{bmatrix}.$$

Associated Jacobian matrix is given by,

$$F = \begin{bmatrix} \rho S & 0 & 0 \\ \beta_1 & 0 & 0 \\ \beta_2 & \gamma_2 & 0 \end{bmatrix}, \text{ and } L = \begin{bmatrix} \beta_1 + \beta_2 + \delta_0 & 0 & 0 \\ 0 & \gamma_1 + \gamma_2 + \delta_0 & 0 \\ 0 & 0 & \mu + r + \delta_0 \end{bmatrix}.$$

At the DFE point, $E_{dfe} \left(\frac{\alpha}{\delta_0}, 0, 0, 0, 0 \right)$, we have

$$F = \begin{bmatrix} \frac{\alpha\rho}{\delta_0} & 0 & 0 \\ \beta_1 & 0 & 0 \\ \beta_2 & \gamma_2 & 0 \end{bmatrix}, \text{ and } L^{-1} = \begin{bmatrix} \frac{1}{\beta_1 + \beta_2 + \delta_0} & 0 & 0 \\ 0 & \frac{1}{\gamma_1 + \gamma_2 + \delta_0} & 0 \\ 0 & 0 & \frac{1}{\mu + r + \delta_0} \end{bmatrix}.$$

Now, it is necessary to assess the next generation matrix G in a manner that,

$$G = FL^{-1} = \begin{bmatrix} \frac{\alpha\rho}{\delta_0(\beta_1 + \beta_2 + \delta_0)} & 0 & 0 \\ 0 & 0 & 0 \\ 0 & 0 & 0 \end{bmatrix}.$$

Now the characteristic equation is given by setting, $|G - \lambda I| = 0$

$$\Rightarrow \begin{vmatrix} \frac{\alpha\rho}{\delta_0(\beta_1 + \beta_2 + \delta_0)} - \lambda & 0 & 0 \\ \frac{\beta_1}{(\beta_1 + \beta_2 + \delta_0)} & -\lambda & 0 \\ \frac{\beta_2}{(\beta_1 + \beta_2 + \delta_0)} & \frac{\gamma_2}{(\gamma_1 + \gamma_2 + \delta_0)} & -\lambda \end{vmatrix} = 0.$$

Hence, the largest eigenvalue of the matrix G is $\frac{\alpha\rho}{\delta_0(\beta_1 + \beta_2 + \delta_0)}$. Thus, the basic reproduction number of the model equation (1) is $R_0 = \frac{\alpha\rho}{\delta_0(\beta_1 + \beta_2 + \delta_0)}$.

With the parameters employed in our simulations (Table 1), using $\beta_1 = 0.139$ we derive, $R_0 = 0.1694$.

Basic Reproduction Number R_0^* at EEP

By employing a similar approach to the one described in the previous section, we can derive the basic reproduction number (R_0^*) at the EEP. In this step, we obtain the matrix for the gain term,

$$J_F = \begin{bmatrix} \rho S^* & \beta_1 & \beta_2 \\ 0 & 0 & \gamma_2 \\ 0 & 0 & 0 \end{bmatrix},$$

and matrix for losses term,

$$J_V^{-1} = \begin{bmatrix} \frac{1}{\beta_1 + \beta_2} & 0 & 0 \\ 0 & \frac{1}{\gamma_1 + \gamma_2} & 0 \\ 0 & 0 & \frac{1}{\mu + r} \end{bmatrix}.$$

Also, next generation matrix, $G = J_F J_V^{-1}$

$$\therefore G = \begin{bmatrix} \frac{\rho S^*}{\beta_1 + \beta_2} & \frac{\beta_1}{\gamma_1 + \gamma_2} & \frac{\beta_2}{\mu + r} \\ 0 & 0 & \frac{\gamma_2}{\mu + r} \\ 0 & 0 & 0 \end{bmatrix} \varphi.$$

At the Endemic equilibrium point (E^*), the process involves calculating the Jacobian matrix and subsequently solving for $\det(G - \lambda I) = 0$, we get only one root of the characteristic equations corresponding to $G(E^*)$ is $\lambda_1 = \frac{\rho S^*}{(\beta_1 + \beta_2)}$. Thus, the basic reproduction number at EEP is

$$R_0^* = \frac{\rho S^*}{(\beta_1 + \beta_2)}, \text{ here } \beta_1 = 0.138; \text{ where } S^* = \frac{\beta_1 + \beta_2 + \delta_0}{\rho}, \text{ here } \beta_1 = 0.139.$$

Using the parameters provided in Table 1, the computation of the basic reproduction number at the Endemic equilibrium point (EEP) yields $R_0^* = 1.5232$. This indicates that the endemic outbreak has not been brought under control worldwide.

Remark 4.1. In the calculation above, we do not consider the natural death rate due to the high fatality rate of MVD.

Table 1: Referred estimated parameters values.

Symbols	Descriptions	Values	Units	Reference
α	Birth rate of the susceptible individuals	0.025	day^{-1}	Estimated
ρ	Exposed rate of the individuals	0.152	day^{-1}	[16]
β_1	The isolation rate of the individuals	0.138 – 0.139	Dimensionless	[14]
β_2	The infection rate of exposed population	0.013	Dimensionless	[14]
φ	The rejoining rate of recovered individuals to susceptible	0.004	day^{-1}	Estimated
γ_1	The rejoining rate of isolation individuals to susceptible	0.127	day^{-1}	Estimated
γ_2	The rate at which isolated individuals get infected	0.329	day^{-1}	Estimated
δ_0	Disease induced death rate	0.09	day^{-1}	Estimated
r	Recovered rate of the infected individuals	0.4027	day^{-1}	Estimated
μ	Natural death rate	0.078	day^{-1}	[4]

Parameter estimation

The non-linear system described in (1) can be utilized to model the actual infection data related to Marburg virus diseases through numerical techniques. Subsequently, we can make accurate forecasts regarding the spread of the disease based on this model. To estimate the parameters in the system of linear differential equations, here we follow these following steps: Convert the system of differential equations into matrix form. Solve the matrix equation by finding the eigenvalues and

eigenvectors of the coefficient matrix. The eigenvalues will give the information about the behavior of the system, while the eigenvectors will provide the solutions. Using the initial conditions or boundary conditions we find the particular solution to the system. Substitute the known values from the particular solution back into the general solution we find the values of the parameters. In some cases, it may not be possible to find exact values for the parameters. In those cases, you can estimate the values using numerical methods such as least squares regression, a methodology elaborated in reference [19, 17].

5 Local Stability Analysis

First, we investigate the stability at disease free equilibrium point S_{dfp} .

Theorem 5.1. *The stability at disease free equilibrium point S_{dfp} of the model equation (1) is locally asymptotically stable if $R_0 < 1$ and unstable if $R_0 > 1$.*

Proof. If we want to proof the theorem at first, we have to find the Jacobian matrix of the model is

$$J = \begin{bmatrix} -\rho E - \delta_0 & -\rho S & \gamma_1 & 0 & \varphi \\ \rho E & \rho S_0 - \beta_1 - \beta_2 & 0 & 0 & 0 \\ 0 & \beta_1 & -\gamma_1 - \gamma_2 & 0 & 0 \\ 0 & \beta_2 & \gamma_2 & -r - \mu & 0 \\ 0 & 0 & 0 & r & -\varphi \end{bmatrix}.$$

At disease free equilibrium, we get $E = 0, S = S_0,$

$$J(W_0) = \begin{bmatrix} -\delta_0 & -\rho S_0 & \gamma_1 & 0 & \varphi \\ 0 & \rho S_0 - \beta_1 - \beta_2 & 0 & 0 & 0 \\ 0 & \beta_1 & -\gamma_1 - \gamma_2 & 0 & 0 \\ 0 & \beta_2 & \gamma_2 & -r - \mu & 0 \\ 0 & 0 & 0 & r & -\varphi \end{bmatrix}.$$

To access the stability of the disease-free equilibrium point, we can establish the characteristic equation for the eigenvalue, λ with $|J(W_0) - \lambda I| = 0,$

$$\Rightarrow \begin{vmatrix} -\delta_0 - \lambda & -\rho S_0 & \gamma_1 & 0 & \varphi \\ 0 & \rho S_0 - \beta_1 - \beta_2 - \lambda & 0 & 0 & 0 \\ 0 & \beta_1 & -\gamma_1 - \gamma_2 - \lambda & 0 & 0 \\ 0 & \beta_2 & \gamma_2 & -r - \mu - \lambda & 0 \\ 0 & 0 & 0 & r & -\varphi - \lambda \end{vmatrix} = 0.$$

Substitute $S_0 = \frac{\alpha}{\delta_0}$ to get,

$$\Rightarrow \begin{vmatrix} -\delta_0 - \lambda & -\frac{\rho\alpha}{\delta_0} & \gamma_1 & 0 & \varphi \\ 0 & \frac{\rho\alpha}{\delta_0} - \beta_1 - \beta_2 - \lambda & 0 & 0 & 0 \\ 0 & \beta_1 & -\gamma_1 - \gamma_2 - \lambda & 0 & 0 \\ 0 & \beta_2 & \gamma_2 & -r - \mu - \lambda & 0 \\ 0 & 0 & 0 & r & -\varphi - \lambda \end{vmatrix} = 0.$$

We get, $\lambda_1 = -\delta_0$, $\lambda_2 = \frac{\rho\alpha}{\delta_0} - \beta_1 - \beta_2 = (R_0 - 1)(\beta_1 + \beta_2)$, where $R_0 = \frac{\rho\alpha}{\delta_0(\beta_1 + \beta_2)}$.

$\lambda_3 = -\gamma_1 - \gamma_2$, $\lambda_4 = -r - \mu$, $\lambda_5 = -\varphi$. Since all eigenvalues are negative when $R_0 - 1 < 0$ i.e. $R_0 < 1$. So, diseases free equilibrium point is locally stable when $R_0 < 1$. □

Theorem 5.2. *The stability at endemic equilibrium point S_{eep} of the model equation (1) is locally asymptotically stable in ϕ if $R_0 > 1$ and unstable if $R_0 < 1$.*

Proof. The proof is as straight-forward as proven in [27]. □

6 Global Stability Analysis

In this section, we aim to demonstrate the conditions for the global asymptotic stability of the disease-free equilibrium point within (\mathbb{R}_5^+) , we use Lyapunov method [7, 8].

Theorem 6.1. *The disease-free equilibrium point of the system described by equation (1) is globally asymptotically stable if $0 < R_0 < 1$ within the feasible region’s interior.*

Proof. In this context, we examine the following nonlinear Lyapunov function,

$$L = S - \bar{S} - \bar{S} \ln\left(\frac{S}{\bar{S}}\right) + E - \bar{E} - \bar{E} \ln\left(\frac{E}{\bar{E}}\right) + I_{nf} - \bar{I}_{nf} - \bar{I}_{nf} \ln\left(\frac{I_{nf}}{\bar{I}_{nf}}\right).$$

Consequently, the derivative of L along the solution curves of the equation (1)–(8) is given by the expression:

$$\begin{aligned} \frac{dL}{dt} &= \frac{dS}{dt} - \frac{\bar{S}}{S} \frac{dS}{dt} + \frac{dE}{dt} - \frac{\bar{E}}{E} \frac{dE}{dt} + \frac{dI_{nf}}{dt} - \frac{\bar{I}_{nf}}{I_{nf}} \frac{dI_{nf}}{dt}, \\ \Rightarrow \frac{dL}{dt} &= \alpha + \gamma_1 I_{so} + \varphi R - \rho S E - \delta_0 S - \frac{\bar{S}}{S} (\alpha + \gamma_1 I_{so} + \varphi R - \rho S E - \delta_0 S) \\ &\quad + (\rho S E - \beta_1 E - \beta_2 E - \delta_0 E) \left(1 - \frac{\bar{E}}{E}\right) + (\beta_2 E + \gamma_2 I_{so} - (r + \mu + \delta_0) I_{nf}) \left(1 - \frac{\bar{I}_{nf}}{I_{nf}}\right). \end{aligned}$$

At the DFE point, putting $\alpha = \delta_0 \bar{S}$, $\bar{E} = 0$, $\bar{I}_{nf} = 0$ yields,

$$\begin{aligned} \frac{dL}{dt} &= \delta_0 \bar{S} \left(1 - \frac{\bar{S}}{S}\right) + \varphi R \left(1 - \frac{\bar{S}}{S}\right) - (\rho E + \delta_0) S \left(1 - \frac{\bar{S}}{S}\right) + \gamma_1 I_{so} \left(1 - \frac{\bar{S}}{S}\right) \\ &\quad - (\beta_1 + \beta_2 + \delta_0) E \left(1 - \frac{\rho S}{(\beta_1 + \beta_2 + \delta_0)}\right) + \beta_2 E + \gamma_2 I_{so} - (r + \mu + \delta_0) I_{nf}, \\ \Rightarrow \frac{dL}{dt} &= \delta_0 \bar{S} \left(1 - \frac{\bar{S}}{S}\right) + \varphi R \left(1 - \frac{\bar{S}}{S}\right) - (\rho E + \delta_0) S \left(1 - \frac{\bar{S}}{S}\right) + \gamma_1 I_{so} \left(1 - \frac{\bar{S}}{S}\right) \\ &\quad - (\beta_1 + \beta_2 + \delta_0) E (1 - R_0) + \beta_2 E + \gamma_2 I_{so} - (r + \mu + \delta_0) I_{nf}. \end{aligned}$$

Considering that all parameter values and variables are positive, it can be inferred that $\frac{dL}{dt} < 0$ for $0 < R_0 < 1$ with $\frac{dL}{dt} = 0$ if and only if the following conditions are met:

$$S = \bar{S}, \quad E = \bar{E} = 0, \quad I_{so} = \bar{I}_{so} = 0, \quad I_{nf} = \bar{I}_{nf} = 0.$$

Hence, we can conclude that the disease-free equilibrium point is globally asymptotically stable when $0 < R_0 < 1$. □

Theorem 6.2. *The endemic equilibrium point (W^*) described by equation (1) is globally asymptotically stable if the basic reproduction number (R_0^*) is greater than 1 within the feasible region’s interior.*

Proof. The mentioned theorem can be demonstrated based on the Lyapunov stability theorem [9, 11]. For this purpose, we contemplate the subsequent nonlinear Lyapunov function:

$$L^* = S - S^* - S^* \ln \left(\frac{S}{S^*} \right) + E - E^* - E^* \ln \left(\frac{E}{E^*} \right) + I_{nf} - I_{nf}^* - I_{nf}^* \ln \left(\frac{I_{nf}}{I_{nf}^*} \right).$$

As a result, the rate of change of L along the solution curves of equation (1) can be represented as:

$$\begin{aligned} \frac{dL^*}{dt} &= \frac{dS}{dt} - \frac{S^*}{S} \frac{dS}{dt} + \frac{dE}{dt} - \frac{E^*}{E} \frac{dE}{dt} + \frac{dI_{nf}}{dt} - \frac{I_{nf}^*}{I_{nf}} \frac{dI_{nf}}{dt}, \\ \Rightarrow \frac{dL^*}{dt} &= \alpha \left(1 - \frac{S^*}{S} \right) + \varphi R \left(1 - \frac{S^*}{S} \right) - (\rho E + \delta_0) S \left(1 - \frac{S^*}{S} \right) + \gamma_1 I_{so} \left(1 - \frac{S^*}{S} \right) \\ &\quad + \rho S E \left(1 - \frac{E^*}{E} \right) - (\beta_1 + \beta_2) E \left(1 - \frac{E^*}{E} \right) + (\beta_2 E + \gamma_2 I_{so} - (r + \mu +) I_{nf}) \left(1 - \frac{I_{nf}^*}{I_{nf}} \right). \end{aligned} \tag{7}$$

At the endemic equilibrium point W^* , we have

$$\alpha = \rho S^* E^* + \delta_0 S^* - \varphi R^* - \gamma_1 I_{so}^*, \tag{8}$$

$$\beta_1 + \beta_2 = \frac{\rho S^* E^*}{E^*}, \tag{9}$$

$$(r + \mu) I_{nf} = \beta_2 E^* + \gamma_2 I_{so}^*. \tag{10}$$

Using these values in (7), we get,

$$\begin{aligned} \frac{dL^*}{dt} &= (\rho S^* E^* + \delta_0 S^* - \varphi R^* - \gamma_1 I_{so}^*) \left(1 - \frac{S^*}{S} \right) + \varphi R \left(1 - \frac{S^*}{S} \right) - (\rho E + \delta_0) S \left(1 - \frac{S^*}{S} \right) \\ &\quad + \gamma_1 I_{so} \left(1 - \frac{S^*}{S} \right) + \rho S E \left(1 - \frac{E^*}{E} \right) - \frac{\rho S^* E^*}{E^*} E \left(1 - \frac{E^*}{E} \right) + \beta_2 E \left(1 - \frac{I_{nf}^*}{I_{nf}} \right) \\ &\quad + \gamma_2 I_{so} \left(1 - \frac{I_{nf}^*}{I_{nf}} \right) - (\beta_2 E^* + \gamma_2 I_{so}^*) \left(1 - \frac{I_{nf}^*}{I_{nf}} \right), \\ \Rightarrow \frac{dL^*}{dt} &= \delta_0 S^* \left(2 - \frac{S^*}{S} - \frac{S}{S^*} \right) + \varphi R \left(1 - \frac{S^*}{S} + \frac{R^* S^*}{RS} - \frac{R^*}{R} \right) + \left(1 - \frac{E^*}{E} \right) (\rho S E - \rho S^* E^*) \\ &\quad + \gamma_1 I_{so} \left(1 - \frac{S^*}{S} - \frac{I_{so}^*}{I_{so}} + \frac{I_{so}^* S^*}{I_{so} S} \right) + \gamma_2 I_{so} \left(1 - \frac{I_{so}^*}{I_{so}} + \frac{I_{so}^* I_{nf}^*}{I_{so} I_{nf}} \right) \\ &\quad + \beta_2 E \left(1 - \frac{E^*}{E} + \frac{I_{nf}^* E^*}{I_{nf} E} \right), \\ \Rightarrow \frac{dL^*}{dt} &= \delta_0 S^* \left(2 - \frac{S^*}{S} - \frac{S}{S^*} \right) + \varphi R \left(1 - \frac{S^*}{S} + \frac{R^* S^*}{RS} - \frac{R^*}{R} \right) + \left(1 - \frac{E^*}{E} \right) (\beta_1 + \beta_2) E (1 - R_0^*) \\ &\quad + \gamma_1 I_{so} \left(1 - \frac{S^*}{S} - \frac{I_{so}^*}{I_{so}} + \frac{I_{so}^* S^*}{I_{so} S} \right) + \gamma_2 I_{so} \left(1 - \frac{I_{so}^*}{I_{so}} + \frac{I_{so}^* I_{nf}^*}{I_{so} I_{nf}} \right) \\ &\quad + \beta_2 E \left(1 - \frac{E^*}{E} + \frac{I_{nf}^* E^*}{I_{nf} E} \right). \end{aligned}$$

Given that the arithmetic mean is greater than or equal to the geometric mean, we have the following relationship,

$$\begin{aligned}
 2 - \frac{S^*}{S} - \frac{S}{S^*} &\leq 0, \\
 1 - \frac{S^*}{S} + \frac{R^* S^*}{RS} - \frac{R^*}{R} &\leq 0, \\
 1 - \frac{S^*}{S} - \frac{I_{so}^*}{I_{so}} + \frac{I_{so}^* S^*}{I_{so} S} &\leq 0, \\
 1 - \frac{I_{so}^*}{I_{so}} + \frac{I_{so}^* I_{nf}^*}{I_{so} I_{nf}} &\leq 0, \\
 1 - \frac{E^*}{E} + \frac{I_{nf}^* E^*}{I_{nf} E} &\leq 0.
 \end{aligned}$$

Further, since all the parameters of the model are non-negative, it follows that $\frac{dL^*}{dt} \leq 0$ for $R_0^* > 1$ with $\frac{dL^*}{dt} = 0$ if and only if $S = S^*, E = E^*, I_{so} = I_{so}^*$ holds. The largest compact invariant set in the feasible region $\frac{dL^*}{dt} = 0$ is the singleton $\{W^*\}$, where W^* is the EEP. In accordance with LaSalle’s invariance principle [4], it can be deduced that W^* is globally stable within the interior of \mathbb{R}_5^+ .

Hence, our model is globally asymptotically stable for $R_0^* > 1$. □

7 Sensitivity Analysis

Sensitivity analysis plays a crucial role in understanding the impact of various parameters in a model. It involves assessing how the uncertainty in the output of a mathematical model, whether numerical or otherwise, can be attributed to different sources of uncertainty in its inputs. Sensitivity analysis is a valuable tool for identifying key parameters that influence disease transmission dynamics. The sensitivity of a parameter is calculated by dividing the percentage change in the model’s output by the percentage change in the parameter itself [5]. This type of analysis aids epidemiologists in pinpointing the critical parameters that need attention for disease prevention. When parameters change, the sensitivity index allows us to calculate the rate of change in variables. In our analysis, We utilize the normalized forward sensitivity index [5, 18] for the basic reproduction number (R_0) with respect to all model parameters.

The standard sensitivity index of R_0^* , that depends partially on a parameter k , is given by,

$$M_{R_0}^k = \frac{k}{R_0} \times \frac{\partial R_0}{\partial k}, \quad \text{for } R_0 \neq 0.$$

Hence, we calculate sensitivity index of R_0^* concerning different model parameters,

$$M_{R_0}^\alpha = \frac{\alpha}{R_0} \times \frac{\partial R_0}{\partial \alpha} = 1.$$

Similarly, we calculate the entire sensitivity index described in Table 2.

$$M_{R_0}^\rho = \frac{\rho}{R_0} \times \frac{\partial R_0}{\partial \rho} = 1,$$

$$M_{R_0}^{\delta_0} = \frac{\delta_0}{R_0} \times \frac{\partial R_0}{\partial \delta_0} = -1,$$

$$M_{R_0}^{\beta_1} = \frac{\beta_1}{R_0} \times \frac{\partial R_0}{\partial \beta_1} = -0.908496732,$$

$$M_{R_0}^{\beta_2} = \frac{\beta_2}{R_0} \times \frac{\partial R_0}{\partial \beta_2} = -0.091503267.$$

Table 2: Sensitivity index associated with each model parameter.

Parameter	Sensitivity index
α	1
ρ	1
δ_0	-1
β_1	-0.908496732
β_2	-0.091503267

A positive sensitivity index for a model parameter indicates that an increase in the parameter will lead to an increase in the basic reproduction number, and vice versa. From the Table 2, we find here the most important parameter of our proposed model are the birth rate of the susceptible individuals (α), the exposed rate of the individuals (ρ), natural death rate (δ_0). The isolation rate of the individuals (β_1) and the infection rate of exposed population (β_2).

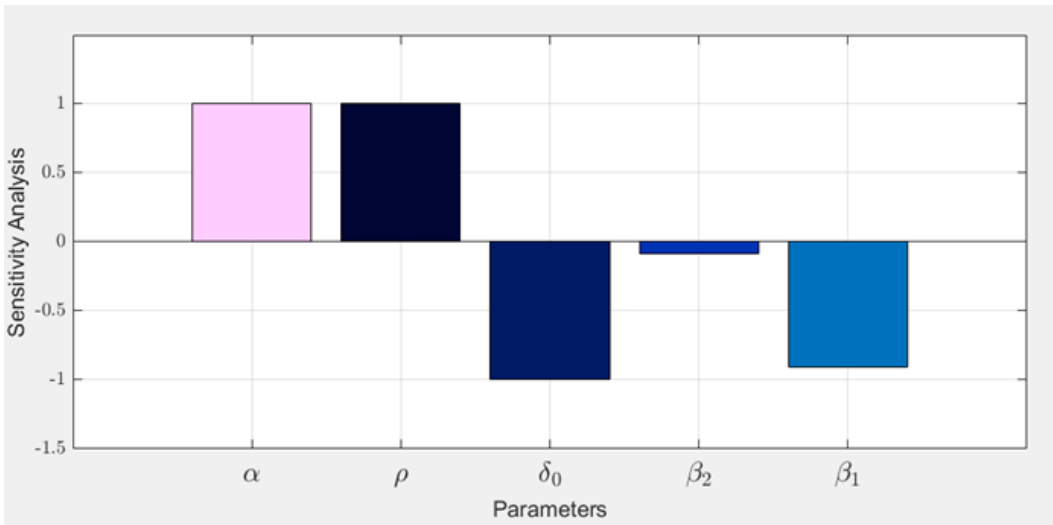


Figure 3: The sensitivity of the reproduction number with respect to all the parameters.

From the above Figure 3, the value 1 indicate that basic reproduction number is directly proportional to α and ρ . So, the transmission rate of the MVD will be decreases if we tracking down the infected individuals and also strictly follow the safety measure. The value $\beta_1 = -0.908496732$

indicate that R_0 is decreases 91% if β_1 is increases 100%. It means if we will be more careful about the rate of isolated individuals then we can control the diseases. And on the other hand, the value $\beta_2 = -0.091503267$ indicate that R_0 is decreases 9% if β_2 is increases 100%. It means if we decrease the infection rate from the exposed individuals diseases can be under control.

8 Numerical Simulation

To estimate the important model parameters using MVD infection cases in Africa from 2000 to 2020, we employ the MATLAB optimization software, *fmincon*. When using the MATLAB package, we consider the initial population size as $S(0) = 2$, $E(0) = 1.7$, $I_{so}(0) = 1.6$, $I_{n,f}(0) = 0.1$ and $R(0) = 0$, where all are estimated in Figures 4 and 5.

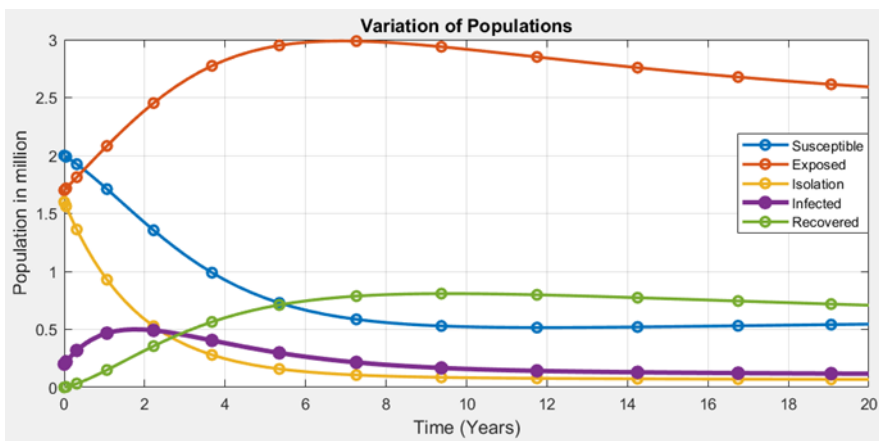


Figure 4: Numerically assess the impact of various model parameters on MVD transmission within the proposed model.

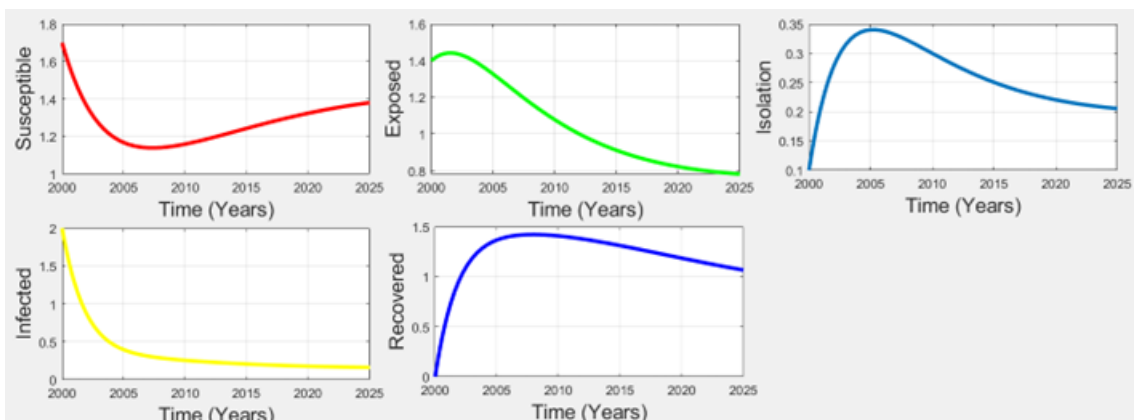


Figure 5: Simulation for MVD infection of the individuals with time (years) when $R_0 < 1$.

Here we observe that, at the early stage, when the number of isolated individuals increases the number of infected individuals monotonically decreases. At the same time the number of exposed individuals also decreases. We also see that, at first, the number of susceptible populations decreases. But after some years, it increases gradually, which suggests that the number of

infected populations decreases and so, the number of susceptible populations increases. In the battle against this formidable foe, the need for a vaccine against MVD looms large. The result helps in estimating the resources needed to manage an outbreak effectively. By predicting the number of individuals likely to be infected or requiring medical care, healthcare resources can be allocated more efficiently. It is imperative to recognize that this represents one of the most effective weapons in our arsenal, and its development should be prioritized to safeguard human health and well-being.

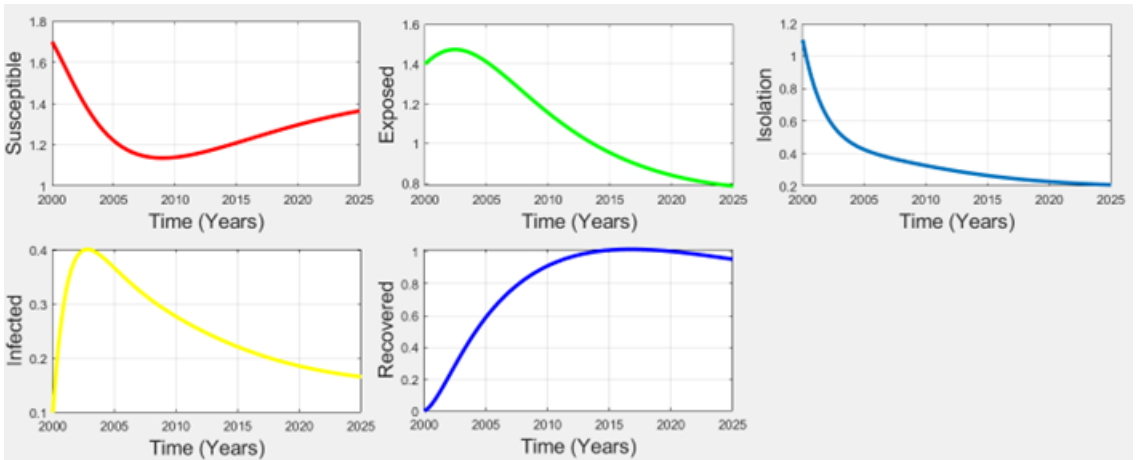


Figure 6: Simulation for MVD infection of the individuals with time (years) when $R_0 > 1$.

From the Figure 6, we can find that when the number of isolated individuals monotonically decreases, the number of infected individuals increases rapidly at first; but later after some years it starts to decrease very fast in the beginning, and then it decreases slowly. The reason for this fact is that when isolated individuals are maintaining all the ruled of hygiene, taking a healthy diet, avoiding junk food items and doing regular exercise, their immune system gets stronger. For this reason, the number of viral infections is less at that moment. Maintaining a healthy weight, while avoiding the pitfalls of alcohol and tobacco, is paramount to shoring up our defenses against MVD and other health threats. Stress, a silent undermine of health, must be managed effectively to ensure a harmonious and resilient immune system.

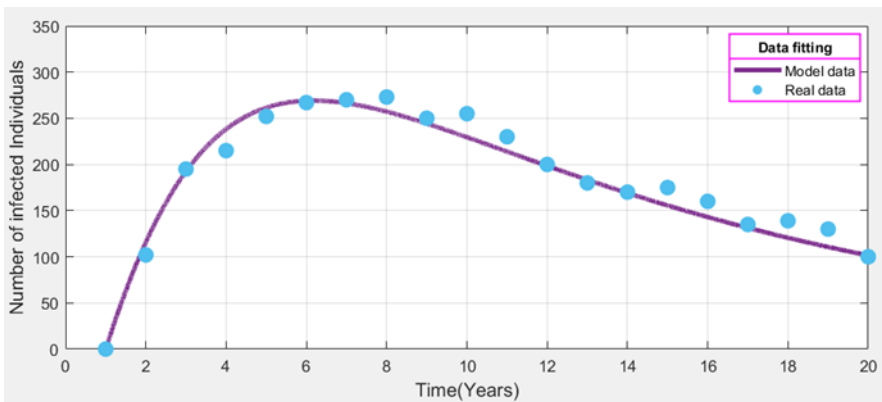


Figure 7: Real data per year (2000 to 2020) in Africa fitting with our proposed model.

Above Figure 7 presented the scenario of infections in Africa from 2000 to 2020 per year. It is seen that the cumulative is flattening after the year 2014 which means that the infection is not increasing and the disease is under control in Africa continent. It's worth noting that our proposed model aligns well with actual reported data from the first wave (spanning from 2001 to 2010). The model exhibits a strong fit with the number of infected individuals in Africa. The study can assist in early detection of potential outbreaks by analyzing data and predicting disease trends. This early warning enables healthcare systems to prepare and respond promptly to mitigate the spread of the virus. At early stage, the disease increases rapidly for not keeping attention of Marburg virus disease. Since the incubation period of this virus is 2 to 21 days. But increasing home quarantine, maintaining proper hygiene and changing food habit and effective exercise for increasing our immunity system strong the infection of this disease is decreased day by day. After some years we can easily see in Figure 7 that this disease is going to be under control. After 2015 it seems that the disease is in a steady state.

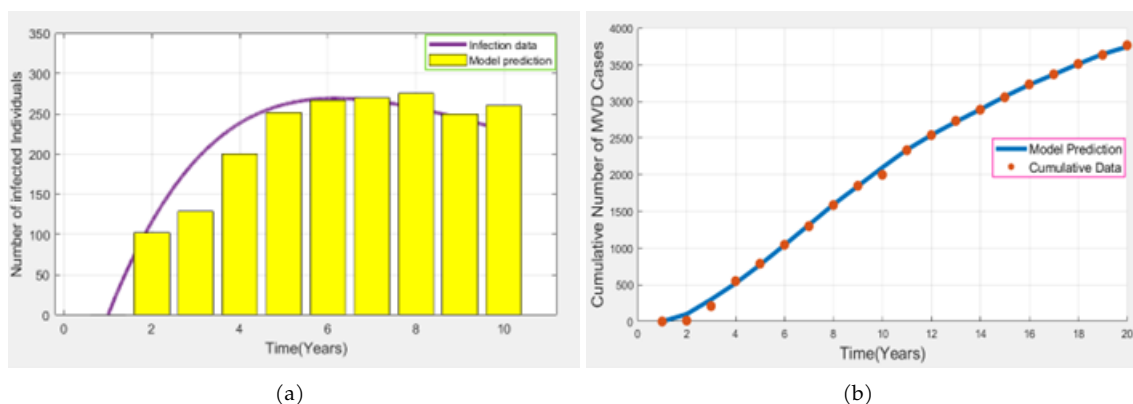


Figure 8: 8(a) Bar diagram represents MVD infected real cases with our predicted model for 10 years in Africa continent from 2000 to 2010. Our proposed model also fitted to the cumulative infected cases in Africa, presented in Figure 8(b) from 2000 to 2020.

Figure 8(a) Bar diagram represents MVD infected real cases with our predicted model for 10 years in Africa continent from 2000 to 2010. Our proposed model also fitted to the cumulative infected cases in Africa, presented in Figure 8(b) from 2000 to 2020.

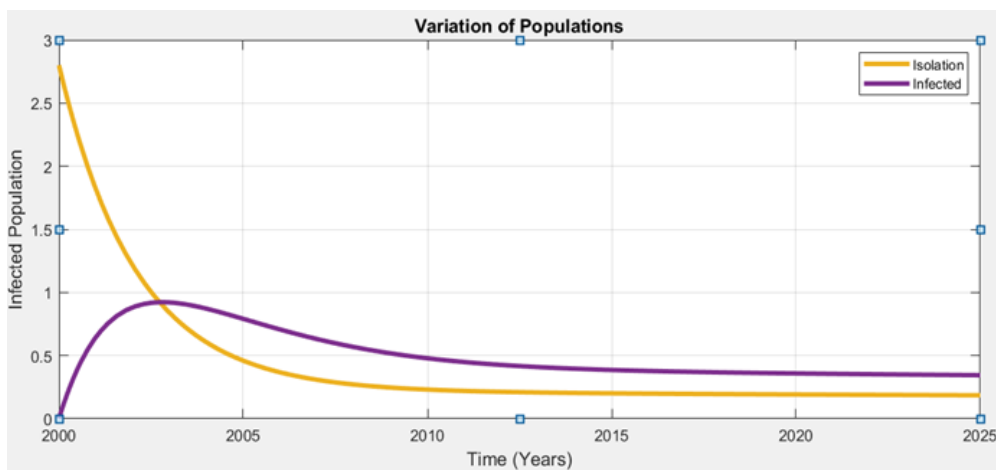


Figure 9: Transmission rate of isolation (β_1) and infected (β_2) individuals together.

Figure 9 defines that when isolation rate will be decreases then infection rate will be increases.

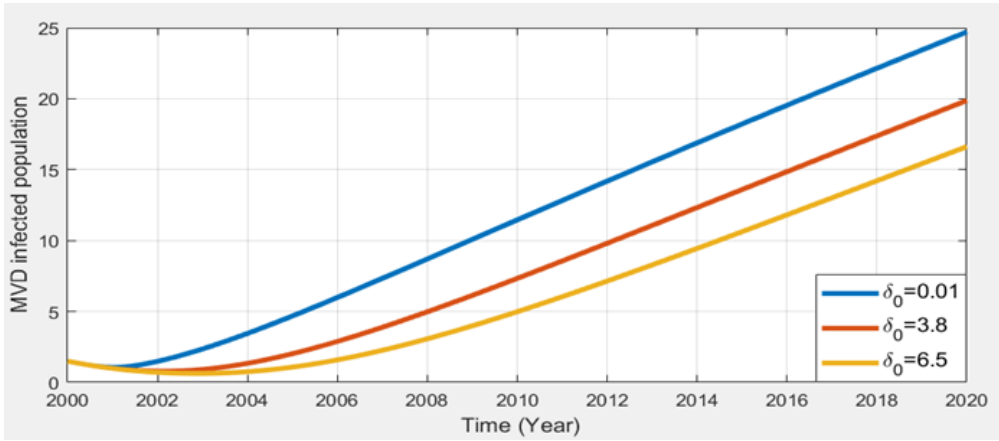


Figure 10: Effect of model parameter δ_0 .

From Figure 10, we observe that if we increase the disease transmission rate is decreasing when natural death rate (δ_0) is increasing.

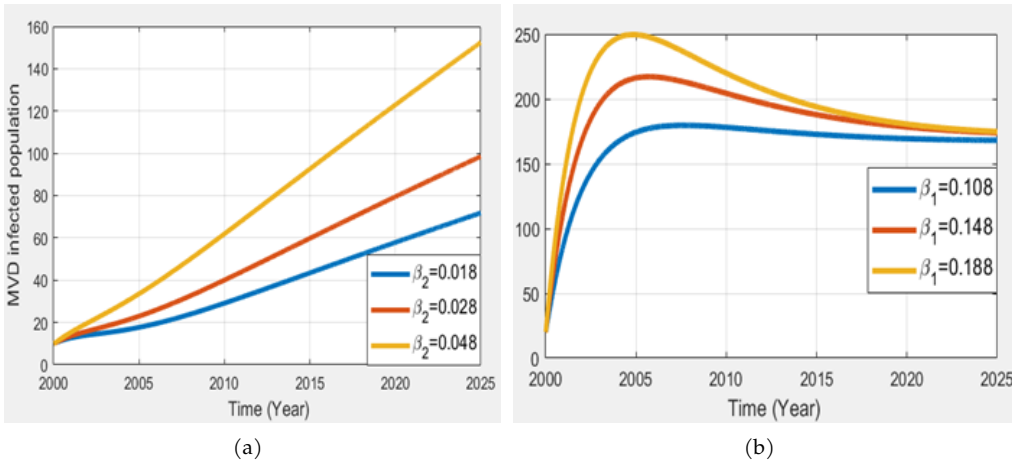


Figure 11: Comparison of the effect of model parameter β_1 and β_2 .

From Figure 11 we have seen that when we increase the rate of isolation individuals the infection is decreasing. Conversely, when we increase the disease transmission rate, it becomes evident that the number of infected individuals increases, and vice versa. This observation indicates that both of these parameters significantly impact the number of infected individuals β_1 and β_2 . Processed foods, which have the potential to undermine the immune system, should be consumed in moderation or eliminated from our diets. Physical activity is not only beneficial for overall health but also plays a pivotal role in enhancing immune function. Adequate and restful sleep is a non-negotiable component of a strong immune system. In the absence of a vaccine, we must rely on our innate defenses, our immune system. To fortify this frontline defense, we must adopt a holistic approach that encompasses lifestyle, dietary, and behavioral changes. A diet rich in fruits, vegetables, whole grains, lean proteins, and healthy fats lays the foundation for a robust immune

system. Staying hydrated through adequate water intake is another cornerstone of good health.

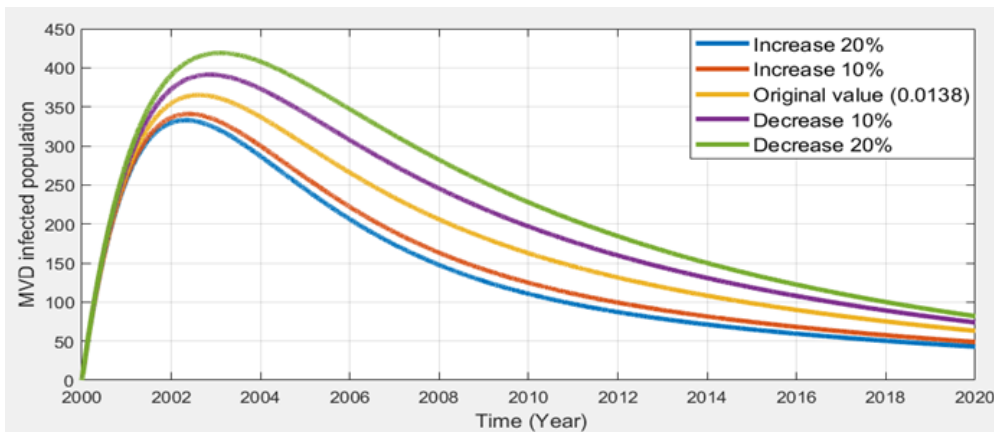


Figure 12: The effect of model parameter β_1 .

Figure 12 shows that increasing the rate of isolation leads to a decrease in MVD infection as it prevents the spread of the virus by limiting contact between infected and non-infected individuals.

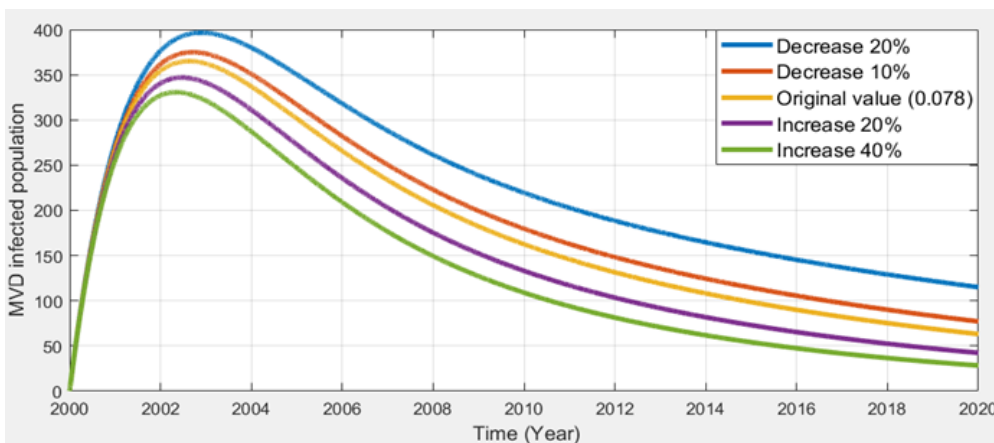


Figure 13: The effect of model parameter β_2 .

From the Figure 13, it is evident that as the infection rate of the exposed population increases, the infection rate of the diseases also increases rapidly. However, after a certain point, the infection rate starts decreasing steadily.

In light of the evolving situation, it is imperative to recognize that the rapid transmission of the virus will become increasingly prevalent over time, especially if the natural death rate and isolation rate continue to decrease. Without the implementation of appropriate measures, this situation may spiral out of control. Our primary focus revolves around a critical parameter: the isolation rate from the exposed population. It has been observed that by effectively isolating individuals from those who have been exposed, we can gradually slow down the rate of infection. Therefore, it becomes evident that the key to maintaining control over the spread of the virus, known as MVD within the human population, lies in taking proactive precautions and enhancing the rate

at which individuals are isolated. Our quest for knowledge and understanding does not stop at the formulation of models. We delve into a meticulous analysis of these models, unearthing vital insights. Through rigorous scrutiny, we ascertain the boundedness and positivity of the model, a crucial step in ensuring its real-world applicability. We delve into the mathematical intricacies of the SEIR model to reveal the underlying stability of the system, primarily through the computation of the basic reproduction number. This number serves as a critical barometer, allowing us to gauge the potential for the virus to establish itself within the population. Furthermore, our analysis unveils the existence of a disease-free equilibrium point within the model. This pivotal discovery emphasizes the urgency of minimizing or eradicating MVD from the human species, and it acts as a catalyst for further research and preventive measures.

In conclusion, vigilance and timely action are of utmost importance to curb the spread of the virus. By bolstering our isolation efforts and practicing stringent preventive measures, we can mitigate the potential for the virus to propagate rapidly, ultimately safeguarding the well-being of our communities.

9 Conclusion

In this comprehensive exploration, we delve into the intricate domain of Marburg Virus Disease (MVD), an ailment that stands as a rare yet ominous threat with the potential to spark devastating epidemics characterized by alarming case fatality rates in Africa. In a world where no approved vaccine or medicine exists to combat this pernicious virus, the safeguard against its wrath is encapsulated in a single word: "precaution." Within the following discourse, we venture into a multifaceted analysis of MVD, culminating in a profound emphasis on the significance of preventive measures. Our journey begins with the formulation of an SEIR (Susceptible-Exposed-Infectious-Removed) epidemic model tailored specifically for MVD within the African context. This model represents an ambitious attempt to encapsulate the intricate web of transmission dynamics, considering all the major parameters at play. Our aim is to gain a deeper understanding of the disease's behavior and dynamics, thereby providing a foundation for informed decision-making. The model's predictions aid policymakers in making informed decisions about implementing specific measures to control the spread of the Marburg virus. It helps in evaluating the trade-offs between different intervention strategies.

To comprehensively grasp the nuances of MVD transmission, we have proposed five distinct compartmental models, each shedding light on a different facet of the disease's progression. These models serve as powerful tools for dissecting and analyzing the potential trajectories of MVD, helping us explore the interplay between various factors and their impact on the spread of the disease. The foundations of our work extend beyond mere theoretical constructs. We validate our findings through sensitivity analysis, which aids in identifying the most influential parameter within the model. In our comprehensive analysis, we employed the normalized forward sensitivity index method and found that the transmission rate from exposed individuals to the isolation compartment emerges as the most critical parameter. This discovery holds significant implications for disease control efforts. As we move from theoretical exploration to practical application, our numerical findings portray a stark reality. In the absence of vaccination or specialized medical treatments, MVD poses a significant challenge. Yet, our simulations offer a ray of hope through enhanced home quarantine and isolation measures. This insight emphasizes the potential for containment and control, emphasizing the importance of collective adherence to these preventive actions.

In conclusion, our extensive study underscores that isolation is currently our most potent weapon against MVD. It serves as a formidable barrier to the virus's spread. However, this is merely a temporary solution. To truly conquer this virulent adversary, we must invest in the development of a vaccine. Simultaneously, we must take charge of our health by adopting measures that enhance our immune system's strength, promoting a healthier, more resilient population. In the absence of a vaccine, our collective actions and adherence to precautionary measures will determine our success in curbing the potential devastation of MVD. Our analysis has yielded important findings. We have observed that the mortality rate associated with MVD increases by a significant 100 percent when an individual's immune system is weakened. This suggests that individuals with compromised immune systems are more susceptible to infection and are more likely to experience severe complications as a result. Moreover, our model demonstrates that increasing the rate of isolation of infected individuals can effectively reduce the concentration of infected individuals in the population. This finding underscores the critical importance of isolation and containment measures in controlling the spread of Marburg virus.

Acknowledgement The author, M. Kamrujjaman research, was partially supported by the University Grants Commission (UGC), and the University of Dhaka, Bangladesh.

Conflicts of Interest The authors declare no conflict of interest.

References

- [1] J. Adjemian, E. C. Farnon, F. Tshioko, J. F. Wamala, E. Byaruhanga, G. S. Bwire, E. Kansiime, A. Kagirita, S. Ahimbisibwe, F. Katunguka, B. Jeffs, J. J. Lutwama, R. Downing, J. W. Tappero, P. Formenty, B. Amman, C. Manning, J. Towner, S. T. Nichol & P. E. Rollin (2011). Outbreak of Marburg hemorrhagic fever among miners in Kamwenge and Ibanda Districts, Uganda, 2007. *The Journal of Infectious Diseases*, 204(suppl_3), S796–S799. <https://doi.org/10.1093/infdis/jir312>.
- [2] C. G. Albariño, T. Shoemaker, M. L. Khristova, J. F. Wamala, J. J. Muyembe, S. Balinandi, A. Tumusiime, S. Campbell, D. Cannon, A. Gibbons, E. Bergeron, B. Bird, K. Dodd, C. Spiropoulou, B. R. Erickson, L. Guerrero, B. Knust, S. T. Nichol, P. E. Rollin & U. Ströher (2013). Genomic analysis of filoviruses associated with four viral hemorrhagic fever outbreaks in Uganda and the Democratic Republic of the Congo in 2012. *Virology*, 442(2), 97–100. <https://doi.org/10.1016/j.virol.2013.04.014>.
- [3] D. G. Bausch, S. T. Nichol, J. J. Muyembe-Tamfum, M. Borchert, P. E. Rollin, H. Sleurs, P. Campbell, F. K. Tshioko, C. Roth, R. Colebunders, P. Pirard, S. Mardel, L. A. Olinda, H. Zeller, A. Tshomba, A. Kulidri, M. L. Libande, S. Mulangu, P. Formenty, T. Grein, H. Leirs, L. Braack, T. Ksiazek, S. Zaki, M. D. Bowen, S. B. Smit, P. A. Leman, F. J. Burt, A. Kemp & R. Swanepoel (2006). Marburg hemorrhagic fever associated with multiple genetic lineages of virus. *New England Journal of Medicine*, 355(9), 909–919. <https://doi.org/10.1056/nejmoa051465>.
- [4] M. H. A. Biswas, M. A. Islam, S. Akter, S. Mandal, M. S. Khatun, S. A. Samad, A. K. Paul & M. R. Khatun (2020). Modelling the effect of self-immunity and the impacts of asymptomatic and symptomatic individuals on COVID-19 outbreak. *Computer Modeling in Engineering & Sciences*, 125(3), 1033–1060. <https://doi.org/10.32604/cmes.2020.012792>.

- [5] N. Chitnis, J. M. Hyman & J. M. Cushing (2008). Determining important parameters in the spread of Malaria through the sensitivity analysis of a mathematical model. *Bulletin of Mathematical Biology*, 70, 1272–1296. <https://doi.org/10.1007/s11538-008-9299-0>.
- [6] H. Feldmann, W. Slenczka & H. D. Klenk (1996). Emerging and reemerging of filoviruses. In *Imported Virus Infections. Archives of Virology Supplement II*, volume 11 pp. 77–100. Springer, Vienna. https://doi.org/10.1007/978-3-7091-7482-1_9.
- [7] M. N. Hassan, M. S. Mahmud, K. F. Nipa & M. Kamrujjaman (2023). Mathematical modeling and COVID-19 forecast in Texas, USA: A prediction model analysis and the probability of disease outbreak. *Disaster Medicine and Public Health Preparedness*, 17, Article ID: e19. <https://doi.org/10.1017/dmp.2021.151>.
- [8] H. F. Huo & L. X. Feng (2012). Global stability of an epidemic model with incomplete treatment and vaccination. *Discrete Dynamics in Nature and Society*, 2012, Article ID: 530267. <https://doi.org/10.1155/2012/530267>.
- [9] M. S. Islam, J. I. Ira, K. A. Kabir & M. Kamrujjaman (2020). Effect of lockdown and isolation to suppress the COVID-19 in Bangladesh: an epidemic compartments model. *Journal of Applied Mathematics and Computation*, 4(3), 83–93. <http://dx.doi.org/10.26855/jamc.2020.09.004>.
- [10] E. D. Johnson, B. K. Johnson, D. Silverstein, P. Tukei, T. W. Geisbert, A. N. Sanchez & P. B. Jahrling (1996). Characterization of a new Marburg virus isolated from a 1987 fatal case in Kenya. In T. F. Schwarz & G. Siegl (Eds.), *Imported Virus Infections. Archives of Virology Supplement II*, volume 11 pp. 101–114. Springer, Vienna. https://doi.org/10.1007/978-3-7091-7482-1_10.
- [11] M. Kamrujjaman, P. Saha, M. S. Islam & U. Ghosh (2022). Dynamics of SEIR model: A case study of COVID-19 in Italy. *Results in Control and Optimization*, 7, Article ID: 100119. <https://doi.org/10.1016/j.rico.2022.100119>.
- [12] F. R. Koundouno, L. E. Kafetzopoulou, M. Faye, A. Renevey, B. Soropogui, K. Ifono, E. V. Nelson, A. A. Kamano, C. Tolno, G. Annibaldis, S. L. Millimono, J. Camara, K. Kourouma, A. Doré, T. E. Millimouno, F. M. Tolno, J. Hinzmann, H. Soubrier, M. Hinrichs, A. Thielebein, G. Herzer, M. Pahlmann, G. A. Ki-Zerbo, P. Formenty, A. Legand, M. R. Wiley, O. Faye, M. M. Diagne, A. A. Sall, P. Lemey, A. Bah, S. Günther, S. Keita, S. Duraffour & N. Magassouba (2022). Detection of Marburg virus disease in Guinea. *New England Journal of Medicine*, 386(26), 2528–2530. <https://doi.org/10.1056/NEJMc2120183>.
- [13] R. J. M. D. Leggiadro (2009). Imported case of Marburg hemorrhagic fever—Colorado, 2008: Centers for disease control and prevention. MMWR. 2009;58 1377–1380. *The Pediatric Infectious Disease Journal*, 29(5), 397–400. <https://doi.org/10.1097/INF.0b013e3181d467bc>.
- [14] M. Martcheva (2015). *An Introduction to Mathematical Epidemiology* volume 61. Springer, New York. <https://doi.org/10.1007/978-1-4899-7612-3>.
- [15] V. V. Nikiforov, I. T. Iu, P. P. Kalinin, L. A. Akinfeeva, L. R. Katkova, V. S. Barmin, E. I. Riabchikova, N. I. Popkova, A. M. Shestopalov & V. P. Nazarov (1994). A case of a laboratory infection with Marburg fever. *Zhurnal Mikrobiologii, Epidemiologii I Immunobiologii*, May-June(3), 104–106.
- [16] OCHA. Uganda monitors 8 after death from Ebola-like Marburg virus. <https://reliefweb.int/report/uganda/uganda-monitors-8-after-death-ebola-marburg-virus> 2014. 6 October 2014, Government of Uganda.

- [17] I. Ratti & P. Kalra (2023). Study of disease dynamics of co-infection of Rotavirus and Malaria with control strategies. *Malaysian Journal of Mathematical Sciences*, 17(2), 151–177. <http://dx.doi.org/10.47836/mjms.17.2.05>.
- [18] U. A. M. Roslan & N. Y. Narayanan (2019). Sensitivity analysis for the dynamics of Leptospirosis disease. *Malaysian Journal of Mathematical Sciences*, 13(S), 77–84. [https://mjms.upm.edu.my/lihatmakalah.php?kod=2019/December/13\(S\)//77-84](https://mjms.upm.edu.my/lihatmakalah.php?kod=2019/December/13(S)//77-84).
- [19] M. A. Safi & S. M. Garba (2012). Global stability analysis of SEIR model with holling type II incidence function. *Computational and Mathematical Methods in Medicine*, 2012, Article ID: 826052. <https://doi.org/10.1155/2012/826052>.
- [20] R. Siegert (1972). *Canine Distemper Virus. Virology Monographs / Die Virusforschung in Einzeldarstellungen*, volume 11, chapter Marburg Virus, pp. 97–153. Springer, Vienna. https://doi.org/10.1007/978-3-7091-8302-1_2.
- [21] D. H. Smith, M. Isaacson, K. M. Johnson, A. Bagshawe, B. K. Johnson, R. Swanapoel, M. Killey, T. Siongok & W. K. Keruga (1982). Marburg-virus disease in Kenya. *The Lancet*, 319(8276), 816–820. [https://doi.org/10.1016/S0140-6736\(82\)91871-2](https://doi.org/10.1016/S0140-6736(82)91871-2).
- [22] A. Timen, M. P. G. Koopmans, A. C. T. M. Vossen, G. J. J. van Doornum, S. Günther, F. Van den Berkmortel, K. M. Verduin, S. Dittrich, P. Emmerich, A. D. M. E. Osterhaus, J. T. van Dissel & R. A. Coutinho (2009). Response to imported case of Marburg hemorrhagic fever, the Netherlands. *Emerging Infectious Diseases*, 15(8), 1171–1175. <https://doi.org/10.3201/eid1508.090015>.
- [23] J. S. Towner, M. L. Khristova, T. K. Sealy, M. J. Vincent, B. R. Erickson, D. A. Bawiec, A. L. Hartman, J. A. Comer, S. R. Zaki, U. Ströher, F. G. da Silva, F. del Castillo, P. E. Rollin, T. G. Ksiazek & S. T. Nichol (2006). Marburgvirus genomics and association with a large hemorrhagic fever outbreak in Angola. *Journal of Virology*, 80(13), 6497–6516. <https://doi.org/10.1128/jvi.00069-06>.
- [24] D. J. Washachi, H. O. Orapine, A. A. Baidu & J. A. Amoka (2022). Mathematical model for the transmission dynamics of Marburg virus diseases with contact tracing and effective quarantine. *FUW Trends in Science & Technology Journal*, 7(3), 35–43.
- [25] WHO (1975). Weekly epidemiological record. *Weekly Epidemiological Record = Relevé Épidémiologique Hebdomadaire*, 50(12), 121–128. <https://iris.who.int/handle/10665/220285>.
- [26] WHO. Case of Marburg haemorrhagic fever imported into the Netherlands from Uganda. https://www.who.int/emergencies/disease-outbreak-news/item/2008_07_10-en 2008. 10 July 2008.
- [27] F. A. Wodajo & T. T. Mekonnen (2022). Mathematical model analysis and numerical simulation of intervention strategies to reduce transmission and re-activation of hepatitis B disease. *F1000Research*, 11, Article ID: 931. <https://doi.org/10.12688/f1000research.124234.1>.